Dear Author,

Please, note that changes made to the HTML content will be added to the article before publication, but are not reflected in this PDF.

Note also that this file should not be used for submitting corrections.

Algal Research xxx (2015) xxx–xxx

Contents lists available at ScienceDirect

Algal Research

journal homepage: www.elsevier.com/locate/algal

Microdevice for studying the *in situ* permeabilization and characterization of *Chlamydomonas reinhardtii* in lipid accumulation phase

P. Bodénès [a,b], F. Lopes [b], D. Pareau [b], O. Français [a], B. Le Pioufle [a]

[a] SATIE, UMR CNRS 8029, ENS Cachan-Université Paris Saclay, 61 av du Pdt Wilson, 94230 Cachan, France
[b] LGPM, EA 4038, CentraleSupélec-Université Paris Saclay, Grande Voie des Vignes, 92295 Chatenay-Malabry, France

ARTICLE INFO

Article history:
Received 4 December 2015
Received in revised form 11 March 2016
Accepted 14 March 2016
Available online xxxx

Keywords:
Chlamydomonas reinhardtii
Pulsed electric fields
Microfluidics

ABSTRACT

Microalgae are considered as a renewable source of lipid-rich biomass feedstock for biofuels due to their high fatty acids content when cultivated in stress conditions (nitrogen starvation). Nevertheless the use of solvents in conventional extraction methods raises important environmental, health and safety issues. The application of Pulsed Electric Field (PEF) to electroporate microalgae is a promising alternative to traditional processes involved in lipid recovery, as it might permeabilize cell membrane, easing the access out of the cytoplasm, and reducing the use of solvents. In order to study the PEF effects on *Chlamydomonas reinhardtii*, we developed a microdevice that allows real time visualization during such electrical solicitation. A high number of electroporation chambers are designed on this biochip to characterize, in real-time, and in parallel, the permeabilization of cells subjected to PEF using the propidium iodide (PI). Several conditions were investigated (pulse energy, pulse duration and electrical field amplitude). Reduced energy consumption, heat effects and electrochemical reactions are obtained when applying short pulses (5 μs) of high electric field (4 to 6 kV·cm^{-1}). Moreover, an increase is observed in cell diameter and lipid content over time in nitrogen stress conditions. The cell sensitivity to the PEF seems to be affected by the cell diameter. Finally, for the first time, lipid droplet redistribution was observed within the cytoplasm during the treatment, showing that 5 μs pulses lead to additional intracellular electroporation effects.

1. Introduction

1.1. Microalgae as a renewable source

Due to their chemical composition (proteins, pigments, starch, fatty acids) algae can be used for food, feed, medical and energy purposes [1,2]. Many algal strains are able to accumulate high amounts of fatty acids as triacylglycerols (TAGs). The accumulation reaches up to 20–50% of their dry weight in certain conditions such as high light intensity and nitrogen limitation stress [3]. Thus, algae are considered as a renewable source of lipid-rich biomass feedstock for biofuels [4]. This generation of biofuels demonstrates high productivity and no competition with food crops in comparison with the 1st and 2nd generations [5].

The overall energy consumption for each step of the production, from algae culture to downstream processes (harvesting, molecules extraction) is a decisive factor on the price of the end product [6]. The environmental impact of each step, regardless of the energetic consumption, is also a key factor [7–9]. Downstream processes, such as, classic mechanical disruption and harvesting methods, are constantly challenged because of their numerous drawbacks. Moreover, extraction methods are generally ineffective when applied on wet intact cells. New technologies have been studied to weaken algal cells prior to wet extraction, including: microwaves [10,11], ultrasounds [10,12] and electrical fields [13]. All these technologies show very low energy consumptions. However, before their use in the algae industry, their improvement at laboratory scale is mandatory. Thus, studies concerning pulsed electric fields (PEF) applied to algae cells are increasing considerably, as this process weakens cell membranes and improves the extraction of soluble compounds, such as, proteins and carbohydrates [14], or large hydrophobic molecules [15].

PEF is broadly used for other applications in biology, *e.g.*, DNA transfection [16], drug delivery into tissue cells [17,18]; and in food processes: treatment of fruit juices [19,20], pasteurization [21,22], sugar

Abbreviations: a.u., arbitrary units; Cm (μF·cm^{-2}), membrane capacitance; DMSO, dimethyl sulfoxide; E (kV·cm^{-1}), Electric field; E_{50} (kV/cm), electric field corresponding to 50% of permeabilization; FDA, fluorescein diacetate; IPA, isopropyl alcohol; Np, number of pulses delivered during a burst of PEF treatment; nPI_0, number of cells stained by PI in an electroporation chamber before treatment; nPI_1, number of cells stained by PI in an electroporation chamber after treatment; $ntot_1$, number of cells counted in an electroporation chamber after treatment; PI, propidium iodide; PEF, pulse electric field; r (m), cell radius; TAGs, triacylglycerols; TAP, medium tris-acetate-phosphate; TAPN-, medium tris-acetate-phosphate depleted in nitrogen; W (kJ·m^{-3}), energy delivered; Δt_{pu} (μs), pulse width; ΔT_{pu} (°C), heating resulting from on pulse; ΔT_{burst} (°C), heating resulting from on burst; $\Delta\Psi_i$ (V), induced trans-membrane voltage; σ (S·m^{-1}), conductivity; θ (°), angular position on the cellular membrane facing the electrodes.

http://dx.doi.org/10.1016/j.algal.2016.03.023
2211-9264/

extraction from beets [16,23] or pigments extraction from potatoes [24]. The use of PEF on microalgae aims several targets: extraction of lipids [15,25–27], pigments [14,28] and proteins [14,29], or lysis of toxic algae [30].

1.2. Electropermeabilization of microalgae

The application of PEF raises the transmembrane potential up to a critical value and in turn induces membrane permeabilization [31] due to creation of pores, their size and reversibility of which depend on the treatment intensity and duration [32]. Thus, depending on the shape, amplitude (E), duration (Δt_{pu}) and number (N_p) of electric field pulses, different effects on algae can be modulated. Parameter values found in the literature are shown in Table 1.

Conditions found in the literature vary considerably (Table 1). Usual pulse duration ranges from several μs to several ms, while the pulse amplitude varies from 1 to 50 $kV \cdot cm^{-1}$ [33]. The achievement of a non-lethal level of poration is dependent on both parameters [18].

1.3. Electroporation parameters

The level of electroporation can be estimated from the Schwan equation (Eq. (1)) [34], which gives the potential ($\Delta\Psi i$) induced on cells submitted to PEF.

$$\Delta\Psi i = -\frac{3}{2}\, r\, E \cos(\theta) \cdot \left(1 - e^{\frac{-\Delta t_{pu}}{\tau}}\right) \quad (1)$$

where r is the cell radius, Δt_{pu} the duration of an electric field pulse, τ the charging time of the cellular membrane and θ the angular position on the cellular membrane facing the electrodes.

The induced potential ($\Delta\Psi i$) required to trigger permeabilization is known to be in the range 0.2–1.5 V for mammalian cells [33]. Algae strains differ in cell radius (r) and cell properties (affecting τ — Eqs. (2) and (3)). These features are paramount for the selection of the electric field intensity E inducing permeabilization (Eq. (1)) [29].

Furthermore, conventional electroporation uses pulses with a longer duration (Δt_{pu}) than the plasma membrane charging time (τ). The membrane charging time (τ), estimated from 0.4 to 1 μs for mammalian cells [35], depends on the membrane specific capacitance (Cm), the cell radius (r), and the medium (σ_{med}), cell wall (σ_{cw}), cell membrane (σ_m) and cytoplasm (σ_{cyto}) conductivities, respectively, as shown in Eq. (2) (deduced from the single shell model [36]) or in Eq. (3) (deduced from the double shell model where the cell wall is considered [37]).

$$\tau = r\, Cm \left(\frac{1}{\sigma cyt} + \frac{1}{2\,\sigma med}\right) \quad (2)$$

$$\tau = r\, Cm \left(\frac{1}{\sigma cyt} + \frac{\sigma med + \sigma cw}{2\,\sigma med\,\sigma cw}\right). \quad (3)$$

The full charge of the membrane requires a duration of the electric field application longer than several times the charging time τ ($\Delta t_{pu} > 5\,\tau$ to reach 95% of the final charge, when considering Eq. (1)).

For this reason, very short pulses ($\Delta t_{pu} < 1$ μs) may lead to cell apoptosis by affecting internal organelles, while the membrane charge does not reach the permeabilization level [38]. It has been shown that longer pulse durations ($\Delta t_{pu} > 1$ μs) can lead to increased pore radius and resealing time [32,39] (time needed for the membrane to recover, if the permeabilization is reversible). Besides, millisecond pulses can be applied in order to weaken the mechanical resistance of the cells, such as, cytoskeleton [40] or cell wall [29]. As shown in Eq. (1), the induced transmembrane potential $\Delta\Psi_i$ is non-homogenous on the cell surface, as it depends on the angle θ of the cell with the applied field direction. This may focus the effect of PEF to a small region of the membrane [41].

1.4. Electroporation side effects

Applying an electric field in a liquid medium may result in undesirable side effects, such as, Joule heating, water electrolysis and redox reactions at the electrodes [42]. The thermal aspect should indeed be considered when applying PEF, as the Joule effect occurs in the conductive medium. The energy delivered during the PEF treatment W (expressed in $J \cdot m^{-3}$), can be expressed thanks to Eq. (4):

$$W = |E|^2\, \Delta t_{pu}\, \sigma \quad (4)$$

where σ is the medium conductivity in $S \cdot m^{-1}$.

By neglecting thermal external exchanges (diffusion, convection), the temperature elevation (ΔT_{pu}) induced by a pulse, due to the Joule effect, can be over-estimated as shown in Eq. (5) [33].

$$\Delta Tpu = \frac{W}{C\,\rho} \quad (5)$$

where $C \cdot (J \cdot m^{-3} \cdot K^{-1})$ is the heat capacity of the medium, and ρ its density.

During the treatment, if the frequency of pulse delivery is too high and does not enable the temperature to decrease between pulses [43], temperature may increase by several dozens of degrees Celsius, affecting cell viability and degrading valuable compounds, such as, lipids, pigments or proteins. To prevent this heating, some studies on microalgae are performed in a low conductivity buffer [28,29] or with a cooling system [15,25]. However, it is well known that the conductivity of the medium increases during PEF treatment because of the leakage of ions out of the cells [26,39], which might enhance the temperature increase.

Water electrolysis may also occur on electrodes. This leads to gas production at the cathode (hydrogen) and at the anode (oxygen). These mechanisms may have many consequences during PEF application, including: interference with the electric field distribution, change in the medium conductivity, generation of reactive oxygen species and evolution of the medium pH close to the electrodes. Finally, both temperature [44] and reactive oxygen species [45] can affect the permeabilization threshold (the electric field needed to open pores in the membrane) of cell membranes.

In this paper, the effects of PEF application on algae will be observed in real time, using a dedicated microdevice [46]. This microdevice allows real time observation of the cell wall behavior and the distribution of internal lipid droplets during and after pulses application [47,48]. Moreover, the efficiency of the treatment is discussed with respect to the energetic cost of the treatment and heating aspects.

Table 1
PEF parameters (pulse duration, electric field, pulse shape) used on several algae strains.

Pulse duration (μs)	Electric field ($kV \cdot cm^{-1}$)	Pulse shape	Pulse number	Strain	Cells diameter (μm)	Study
1	23–43	Square	20–110	*Auxenochlorella protothecoides*	5–8	[26]
6–150	10–25	Square	50	*Chlorella vulgaris*	2–4	[28]
10	20	Exponential decay	1–600	*Nannochloropsis*	2–3	[14]
100	2.7	Square	21	*Chlorella vulgaris*	2–4	[27]
2 000	3	Square bipolar	30	*Chlorella vulgaris*	2–4	[29]

Please cite this article as: P. Bodénès, et al., Microdevice for studying the *in situ* permeabilization and characterization of *Chlamydomonas reinhardtii* in lipid accumulation phase..., Algal Res. (2015), http://dx.doi.org/10.1016/j.algal.2016.03.023

2. Material and methods

2.1. Microalgae culture

Algae strains were obtained from the Culture Collection of Algae at the University of Goettingen (EPSAG, Nikolausberger Goettingen, Germany). Cultures assessed in this investigation were: *Chlamydomonas reinhardtii* SAG 34.89 (wild type), *C. reinhardtii* SAG 83.81 (Cell wall deficient mutant strain from the wild type 34.98). *C. reinhardtii* wild type and the mutant were cultivated in TAP Medium [49] for the growth phase and in TAP nitrogen depleted medium for the lipid accumulation (NH_4Cl removed from the TAP medium).

2.1.1. Culture conditions

Cells were cultivated photo-autotrophically in exponential growth in 250 mL Erlenmeyer flasks with a culture volume ranging from 20 to 60 mL: rotation speed 150 rpm, temperature 25 °C, enriched air 1.5% CO_2, white light 20 μmol·m^{-2}·s^{-1} at the surface of the flasks. In the exponential phase, microalgae concentrations ranged from $5 \cdot 10^4$ to $5 \cdot 10^7$ cells·mL^{-1}.

In order to trigger the accumulation of neutral lipids in algae cells, the cells were centrifuged (6000 g, 6 min) and resuspended, at a concentration of $2 \cdot 10^6$ cells·mL^{-1} in a 40 mL TAP nitrogen depleted medium. The following conditions were applied: light intensity of 150 μmol·m^{-2}·s^{-1}, agitation at 50 rpm, temperature set at 24 ± 1 °C, 0.0035% CO_2. Cell concentration ranges from $2 \cdot 10^6$ cells·mL^{-1} to $1 \cdot 10^7$ cells·mL^{-1}. In terms of dry weight, the amount of biomass after 7 days of stress was 1.23 ± 0.06 g·L^{-1} for $7.6 \cdot 10^6$ cells·mL^{-1}.

2.2. Microalgae characterization

Cell concentration (in cell·mL^{-1}) was monitored using the Guava easyCyte 5 flow cytometer (Millipore Corporation 25801 Industrial Blvd Hayward, CA 94545). The analysis method was developed on Incyte 2.7 using the following parameters: Forward Scatter gain = 8; Side Scatter gain = 8; RED gain (680 nm) = 8; 5 decades acquisitions; total counts = 2000 events; flow rate = 0.59 μL·s^{-1}.; cell concentration for analyses: from 1 to $3 \cdot 10^5$·cell·mL^{-1}; Forward Scatter threshold: $2 \cdot 10^2$ a.u.; *C. reinhardtii* gate: Forward Scatter from $3 \cdot 10^2$ to $2 \cdot 10^4$ a.u. and Side Scatter from $2 \cdot 10^2$ to $2 \cdot 10^4$ a.u.; threshold on RED fluorescence at $3 \cdot 10^1$ a.u.

Cell size measurements were performed using an inverted microscope Nikon Eclipse Ti–U, with a 40 × magnification objective (Nikon Achromat LWD 40 × Ph1 ADL NA = 0.6) and a CMOS colored camera Nikon DS-Ri2 (4908 × 3264 pixels, 36 × 23.9 mm) equipped with an additional 2.5 × magnification lens. Cell diameter (220 ± 20 cells) was measured manually from bright field images using the camera software NIS-Elements D 4.30. The mean cell size (referred in Fig. 3) is defined as the longest diameter of the spheroidal shaped cells.

To follow the neutral lipid content, Bodipy 505/515 (Lifetechnologies, D-3921) was used to stain lipid droplets in the cell cytoplasm. Bodipy was diluted in DMSO to a concentration of 100 mg·L^{-1}. Then 10 μL of the stock solution was added to 10^6 cells·mL^{-1} (final concentration of 1 μg·mL^{-1}). Stained cells were incubated by rotative mixing in the dark during 10 min. The cells were then centrifuged at 2415 g for 5 min and resuspended in a TAP medium depleted in nitrogen.

The accumulation of Bodipy-stained lipid droplets was monitored using the Guava easyCyte 5 flow Cytometer (Millipore Corporation 25801 Industrial Blvd Hayward, CA 94545). The following analysis method is used to gate *C. reinhardtii* cells: The mean Bodipy fluorescence was estimated on a green detector 525/30 nm (Green gain = 1) from gated *C. reinhardtii* cells. The green autofluorescence value (fluorescence without Bodipy) was subtracted from the mean fluorescence value. Confocal scanning laser microscopy (CLSM) confirmed that Bodipy stained exclusively the lipid droplets and not the phospholipids of the cytoplasmic membrane, as previously reported [50].

2.3. Pulse generator

The experiments were performed using a pulse generator Betatech Electrocell B10 HVLV. The generator parameters were: U = −1000 V to +1000 V (bipolar pulses), Δt_{pu} = 5–50,000 μs (pulse duration), T_i = 5–50,000 μs (duration between positive and negative pulse), P = 80–9999 500 μs (period of one pulse cycle), burst of pulses: 1–10,000 pulses.

2.4. Device microfabrication

The biodevice was designed to trap microalgae cells in visualization chambers. Those chambers were made of thick photoresist, as detailed hereafter, and were patterned above a parallel electrode network. Cells were monitored by microscopy during and after application of pulse electric fields in bright or fluorescence fields. The biochip consisted of two layers: an electric layer to deliver pulsed electric fields and a fluidic layer to trap the cells. It was fabricated using a conventional microfabrication process in a clean room [51].

For the electrodes, a 20 nm chromium adhesion layer, covered by 150 nm gold layer, was sputtered on a quartz substrate. A first photolithography step was employed to pattern the electric layer. This process includes the deposition of S1805 Shipley photoresist by spin coating (t = 30 s, v = 1000 rpm), followed by a prebake (T = 115 °C, t = 1 min) and UV exposure (365 nm, intensity = 120 mJ·cm^{-2}) (Fig. 1a). A developing step was then performed (developer 351, t = 1 min) (Fig. 1b), followed by gold etching with KI (4 g KI, 1 g I_2, 40 mL H_2O, t = 7 s) and chromium etching (ChromeEtch18 micro resist technology, t = 45 s) (Fig. 1c). A cleaning step was done using acetone and isopropanol (IPA).

The microfluidic level was patterned with a second photolithography step: the 25 μm high microfluidic chamber was defined by negative thick photoresist (SU8 2025, Microchem©) spin coated in two steps: t1 = 5 s, v1 = 500 rpm and t2 = 30 s, v2 = 2700 rpm. A soft-baking (t = 3′ at 65 °C and t = 15′ at 95 °C), followed by UV exposure (365 nm, intensity = 240 mJ·cm^{-2}) (Fig. 1d) gave the pattern for the microdevice design (Fig. 1e). A post exposure bake was then done (t = 3′ at 65 °C and t = 15′ at 95 °C) before development (MicroChem © SU8 developer, t = 6 min) associated to a hard-baking step (T = 175 °C, t = 30′, slope 5 °C·min^{-1}) to fix the thick resist level (3 h).

The electrode gap was small enough to reach very high electric fields [46], up to 30 kV·cm^{-1} or 60 kV·cm^{-1} with a gap of 300 μm or 150 μm using an accessible voltage generator (up to 1 kV). The microfluidic layer was designed as a set of 6 lines of 15 chambers for a total of 90 closed chambers (Fig. 2a). There were 3 lines of 45 large chambers (gap of 300 μm) or 3 lines of 45 smaller chambers (gap of 150 μm). Each large chamber had an internal dimension of 720 μm × 480 μm, designed to be observed with a 20 × objective. Small chambers possessed an internal dimension of 360 μm × 150 μm designed for observation with a 40 × objective.

The electroporation microdevice was connected to the pulse generator by a homemade supporting base fastened above the microscope objectives and designed to support up to 2 kV DC voltage (Fig. 2b).

2.5. Characterization of the permeabilization

Cell permeabilization was characterized using propidium iodide (PI). This molecule of 668 Da is an intercalating agent that binds to the DNA of permeable cells. It exhibits excitation and emission peaks of respectively 536 and 617 nm. When the cell is electroporated, the PI molecules can diffuse through the permeable membrane and stain their DNA, while intact cells remain unstained. PI was dissolved in a PBS buffer at a concentration of 1.5 mM and diluted in the sample of microalgae

Please cite this article as: P. Bodénès, et al., Microdevice for studying the *in situ* permeabilization and characterization of *Chlamydomonas reinhardtii* in lipid accumulation phase..., Algal Res. (2015), http://dx.doi.org/10.1016/j.algal.2016.03.023

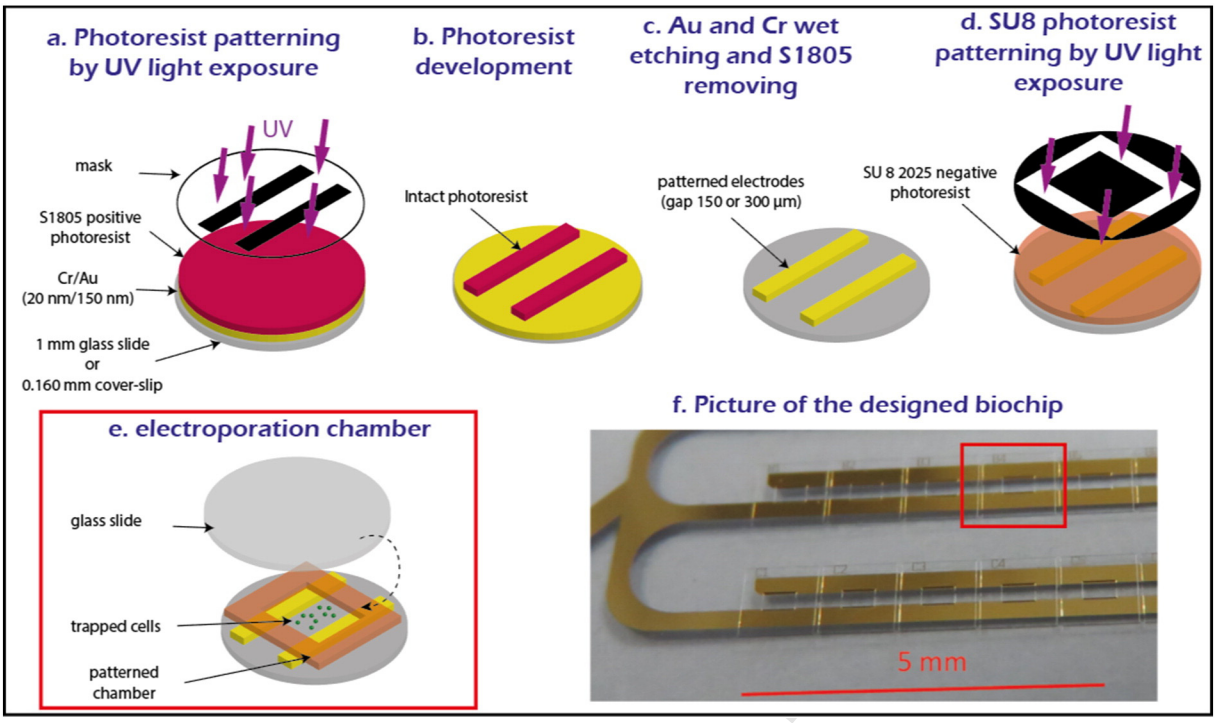

Fig. 1. Microfabrication process of the biodevice. The electrode layer is patterned on a glass substrate in 3 steps: photoresist patterning by UV light exposure (a), photoresist development (b), and Au/Cr wet etching and photoresist removing (c). A fluidic layer is patterned above the electrode layer by a second UV light exposure (d) to obtain several multiple electroporation chambers shown on the scheme (e) and picture (f).

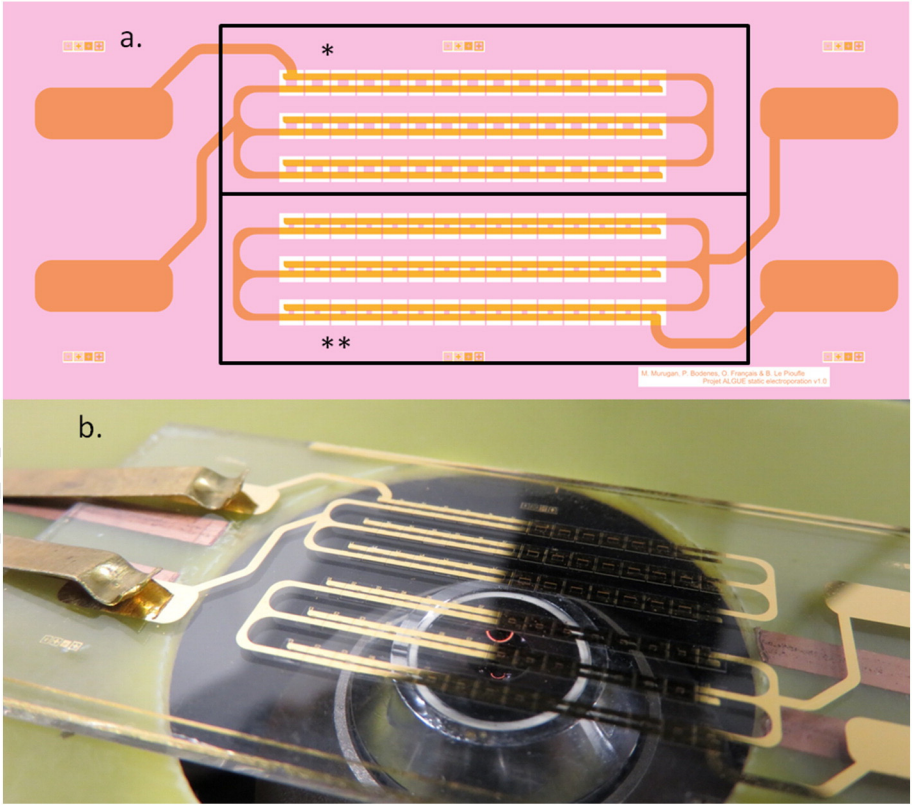

Fig. 2. a. Scheme of the overall design of the electroporation micro-system. Orange: electric level, white: fluidic level. (*) 45 large chambers (internal dimensions: 720 µm × 480 µm, electrode gap: 300 µm) designed to be observed with a 20 × objective, (**) 45 small chambers (internal dimensions: 360 µm × 150 µm, electrode gap: 150 µm) designed to be observed with a 40 × objective. b. Picture of the chip connected to the generator, placed above a microscope objective.

Please cite this article as: P. Bodénès, et al., Microdevice for studying the *in situ* permeabilization and characterization of *Chlamydomonas reinhardtii* in lipid accumulation phase..., Algal Res. (2015), http://dx.doi.org/10.1016/j.algal.2016.03.023

cells (with a cell concentration of $2 \cdot 10^6$–$1 \cdot 10^7$ cells·ml^{-1}) to a final concentration of 100 μM. Then 15 μL of this sample was placed on the surface of the device.

A glass slide (24 mm × 30 mm, d = 1 mm) covered the droplet (15 μL) of algae solution, spreading it in a way that it filled multiple electroporation chambers. All experiments were performed using TAP culture medium. The medium conductivity was 0.213 S·m^{-1} at 20 °C.

The microscopic observations were conducted with a Nikon eclipse Ti-U inverted microscope using a 20× objective (Nikon Plan fluor 20 × DIC N2 NA = 0.6) 40× objective (Nikon Achromat LWD 40× Ph1 ADL NA = 0.5).

Three chambers were utilized for the quantitative analysis of PI penetration. First, the cells in the chambers were observed with a 20× objective and the images were recorded using bright field mode (no fluorescence filter, exposure time of 10 ms and gain 1) and CY3 fluorescence (exposure time of 700 ms, and gain 4). The ratio of the number of stained cells before the PEF treatment and the total number of cells within the chamber was calculated. PEF treatment was then applied. It was observed that PI penetrated permeabilized cells within a few seconds. The counting of permeabilized cells was done, more than 30 s after the treatment, to let treated cells settle down within the focus of the objective. As in the previous treatment, bright field and fluorescent images were recorded, respectively, in order to estimate the total number of cells and finally the percentage of permeabilized cells in the chambers.

It should be pointed out that some cells might be naturally permeabilized because of adverse culture conditions or natural mortality. In the calculation of the PI uptake (Eq. (9)), for each measurement, the total number of cells stained by PI before treatment (nPI_0 consisting of naturally permeabilized cells) were subtracted from the stained cell number after treatment (nPI_1). The total cell number counted in the bright field ($ntot_1$) was also taken into account in the calculation, as shown in Eq. (9).

$$\text{PI uptake}\ (\%) = \frac{nPI1 - nPI0}{ntot1 - nPI0} \times 100. \quad (9)$$

The average number of cells per chamber was approximately 60. PI uptake estimation is calculated on 3 independent chambers and in duplicate experiments.

2.6. Permeability and viability tests in electroporation cuvettes

Additional measurements were performed in 1 mm electroporation cuvettes (Dutscher, ref. 4905020) in order to assess cell viability after electroporation treatment. Viability was monitored using Fluorescein Diacetate (FDA, Thermo fisher scientific F1303) dye that measures cell enzymatic activity. This non-fluorescent dye, after diffusing through the cell is hydrolysed by esterase enzymes and releases fluorescein (which exhibits excitation and emission peaks of respectively 430 nm and 525 nm). Additionally, the cytoplasmic membrane must be intact in order to retain the fluorescent dye inside the cell [52,53]. The following staining protocol was applied: FDA diluted in acetone (final concentration of 5.5 μM, 6 min of incubation) was added to an algae solution ($1–2 \cdot 10^5$ cells·mL^{-1}). FDA positive and negative cells were distinguished by flow cytometry at 525 nm.

Cell permeabilization after PEF treatment was measured using Sytox Green (SG, Thermo fisher scientific S7020), that binds to the DNA of permeabilized cells. This dye and propidium iodide present similar molecular weights (SG: 660 Da, PI: 668 DA [54]). Sytox green (ratio of 1 μmol SG to $1 \cdot 10^5$·cells, 5 min of incubation) is added to an algal solution before PEF treatment. Permeabilized cells were thereafter counted by cytometry at 583 nm.

3. Results and discussion

In the present study, the effect of PEF on *C. reinhardtii* cells accumulating lipids is characterized and quantified using a dedicated microdevice. The increase in cell size over time, in the lipid accumulation phase, was first evaluated (Fig. 3), as this parameter directly influences the level of permeabilization. The cell lipid content was thereafter measured.

3.1. Evolution of microalgae cell size and lipid content in stress conditions

The mean cell diameter in exponential growth was 6.8 ± 1.4 μm, which increased to 9.2 ± 1 μm after 4 days of stress and then was constant at 10 ± 1 μm between day 7 and day 15 (Fig. 3). This is in agreement with results reported by [55] that mentioned a diameter increase of 2 μm (from 5.7 to 7.2 μm) after 96 h of nitrogen stress for the wild type strain *Clamydomonas* CC124. No further increase in the

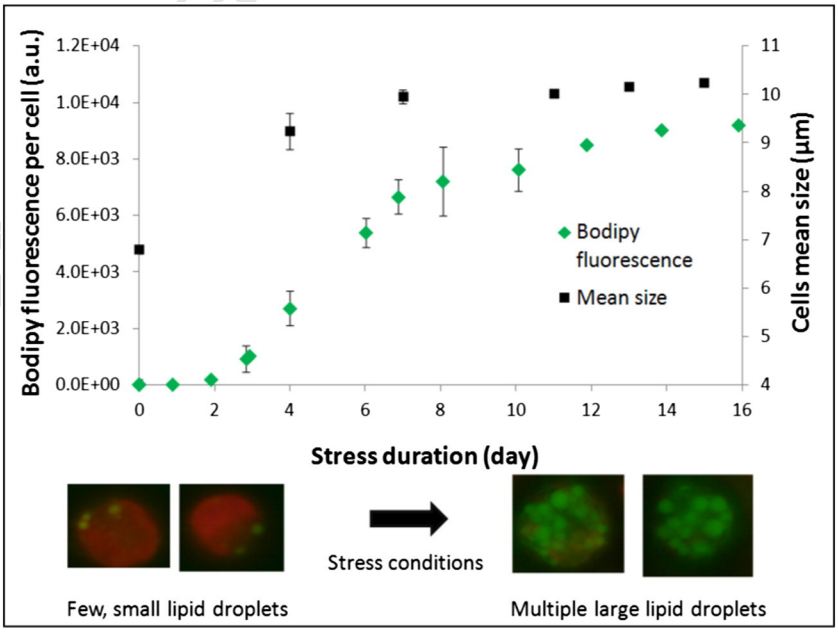

Fig. 3. Evolution of cell lipid content with time. Mean green fluorescence evaluated by flow cytometry.

Please cite this article as: P. Bodénès, et al., Microdevice for studying the *in situ* permeabilization and characterization of *Chlamydomonas reinhardtii* in lipid accumulation phase..., Algal Res. (2015), http://dx.doi.org/10.1016/j.algal.2016.03.023

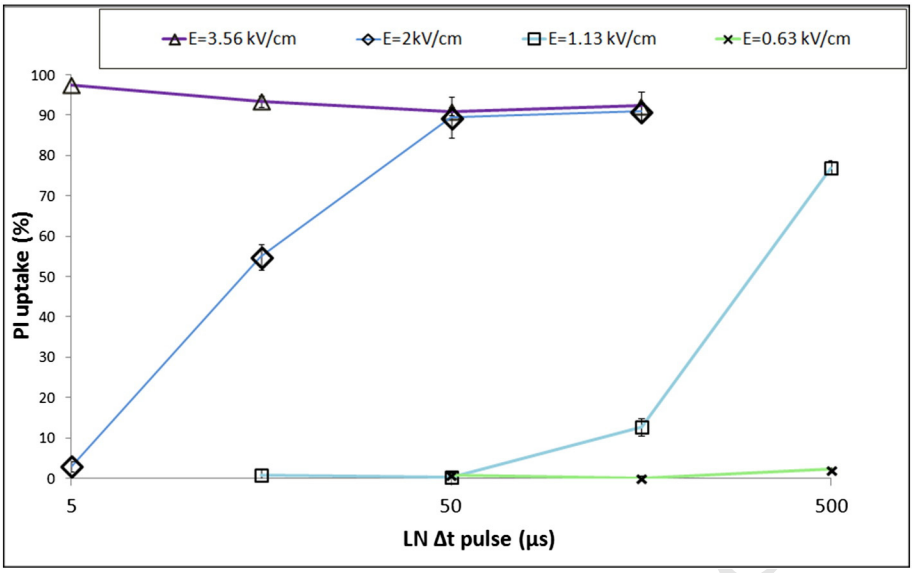

Fig. 4. PI uptake (%) resulting from several treatments with different electric fields E (0.63, 1.13, 2 and 3.56 kV·cm^{-1}) and pulse durations Δt_{pu} (5, 16, 50, 158 and 500 µs). Experiments performed with *Chlamydomonas reinhardtii* cells with 7–8 days of lipid accumulation.

cell diameter is observed after 7 days. This may be due to the presence of a cell wall, which seems to prevent cell swelling, as previously reported [56].

The evolution of lipid content in the cells was followed from day 0 (beginning of the stress) to day 16 (Fig. 3). The lipid content clearly increased during stress (nitrogen starvation).

From the previous observations, we can assume that lipid droplet accumulation started after 3–4 days of stress, which is in agreement with many results of the literature [57]. The lipid accumulation rate seems to decrease after 8 days of stress.

Moreover, data showed that nitrogen related stress induced a diameter increase in *C. reinhardtii*, mostly in the first 4 days, followed by a strong increase of the lipid content from day 4 to day 8. Therefore, we conclude that 8 days of stress correspond to the best time to submit cells to PEF for lipid extraction.

3.2. Effect of the PEF parameters on the electroporation level

We first investigated the relation between the PEF spent energy, for a given level of pulse duration, and the efficiency of the treatment estimated by the propidium iodide uptake. The electric field amplitude was therefore adapted for five pulse durations Δt_{pu} (5, 16, 50, 158 and 500 µs), in order to achieve different levels of energy (135, 426, 1243 kJ·m^{-3}). Joule heating corresponding to each situation was overestimated (cooling not considered) using Eqs. (4) and (5) (Section 1.4). For each treatment, the heat effect ΔT, in °C, was calculated for one pulse (ΔT_{pu}).

All experiments were performed using a burst of 10 Hz monopolar pulses on *C. reinhardtii* SAG 34.89 (wild type) in 7 to 8 days of lipid accumulation (the optimal treatment time determined previously (Section 3.1)).

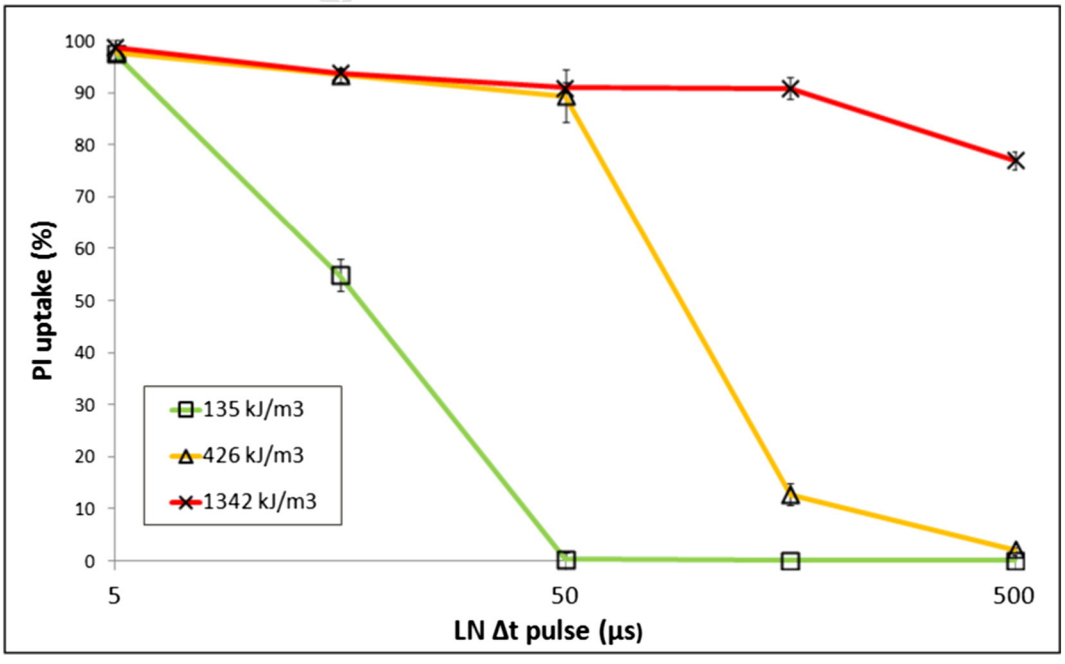

Fig. 5. PI uptake (%) resulting from several treatments varying electric field E (from 0.36 to 20 kV·cm^{-1}) and pulse duration Δt_{pu} (5, 16, 50, 158 and 500 µs) corresponding to 3 levels of energy: 135, 426 and 1342 kJ·cm^{-3}. Experiments performed with *Chlamydomonas reinhardtii* cells with 7–8 days of lipid accumulation.

Please cite this article as: P. Bodénès, et al., Microdevice for studying the *in situ* permeabilization and characterization of *Chlamydomonas reinhardtii* in lipid accumulation phase..., Algal Res. (2015), http://dx.doi.org/10.1016/j.algal.2016.03.023

Table 2
Pulse duration and the corresponding electric field inducing 50% of permeabilization (E_{50}) determined for *Chlamydomonas reinhardtii* (in 7–8 days of lipid accumulation phase).

Pulse duration Δt_{pu} (μs)	500	50	5
E_{50} (kV·cm^{-1})	1.12	2	3.5
Treatment energy W (kJ·m^{-3})	1342	426	135
Increase in temperature ΔT_{pu} (°C)	0.32	0.10	0.03

The results of permeabilization at four levels of electric fields E, and for several treatment durations Δt_{pu}, are presented in Fig. 4, while those for several levels of energy W with respect to the pulse duration Δt_{pu} are presented in Fig. 5.

Considering the Schwan equation (Eq. (1)), the critical electric field that induces electroporation is evaluated to be within the range of 0.3–2.0 kV·cm^{-1} for a cell radius of 5 μm. The charging time τ is within the range of 0.1–0.9 μs (calculated from Eqs. (2) and (3) in which σ_{cyt} depends on the number of lipid droplets in the cytoplasm [36]). Indeed experimental results (Fig. 4) confirm that the minimal electric field required to obtain cell permeabilization is in the range of 1–2 kV·cm^{-1} for the longer pulses ($\Delta t_{pu} > 16$ μs). Pulses of 5 μs require higher electric field (above 2 kV·cm^{-1}) to permeabilize the cells in order to compensate the charging time of the membrane.

In addition, the electric field inducing 50% of cell permeabilization (E_{50}) depends on pulse duration (Table 2).

The obtained electric fields (Table 2) were lower than those reported in the literature, regardless of the applied pulse duration (Table 1, Section 1.2). Indeed, for $\Delta t_{pu} = 5$ μs, values of 10–20 kV·cm^{-1} have been reported [14,28]. Moreover, cell electroporation has been reported at 2.7 kV·cm^{-1} for $\Delta t_{pu} = 100$ μs [27], while our results demonstrate 50% cell permeabilization for a pulse duration between 50 and 500 μs at 1–2 kV·cm^{-1}. Finally, by extrapolating our results, approximately 5–6 kV·cm^{-1} for 1 μs pulse (instead of 23–43 kV·cm^{-1} [26]) and 0.8–0.9 kV·cm^{-1} for 2 ms pulses (instead of 3 kV·cm^{-1} [29]) would be required to induce cell electroporation.

We can easily explain those differences by at least two reasons: (*i*) *C. reinhardtii* cells are 3 to 4 fold larger than *Chlorella vulgaris* and *Nannochloropsis*. This increase in cell diameter contributes to the reduction of the permeabilization threshold by a factor of 3–4 fold according to the Schwan equation (Eq. (1), Section 1.3) and (*ii*), in most cases, including references [26,29], the intensity of the field that is actually applied for algae electroporation is set much higher (2–3 times) than the necessary E_{50} in order to ensure the permeabilization of 100% of the cells.

Fig. 5 shows that, for a similar level of cell permeabilization, more energy is used for long pulses. For instance, 1342 kJ·m^{-3} energy is delivered, using 10 pulses of 500 μs, to permeabilize more than 50% of the cells. Nevertheless, shorter pulses require higher electric field to trigger permeabilization (Table 2 and Eq. (4), Section 1.4). Interestingly, by reducing the pulse duration by 10 times, the electric field is only increased by a factor slightly less than two. Under these conditions, the energy needed for cell electroporation is drastically reduced by a factor of 3.15 (Table 2). Moreover, since the temperature increase is proportional to energy, little heat production is generated when using short pulses with optimized electric field, as demonstrated by our data (Table 2). It should be pointed out that the temperature increase of the entire treatment ΔT_{burst} after 10 pulses, remains close to the temperature increase corresponding to one pulse ΔT_{pu}, due to the natural cooling that occurs between pulses under our frequency conditions and with the large surface to volume ratio [46]. Indeed, simulations showed that for any treatment condition, in our system, the cooling time is shorter than 0.1 s. Nevertheless, this approximation should be reconsidered when using frequencies higher than 10 Hz.

Moreover, it should be noted that for high energy treatments (W ≥ 1342 **kJ·m^{-3}**), gas appeared at the vicinity of electrodes, probably due to water electrolysis or redox reactions. Reducing the energy used during the PEF treatment is thus a way to avoid such effects.

With our conditions (10 pulses), the optimal parameters (inducing high permeabilization for *C. reinhardtii* after 7 days of stress with a low energy consumption) were obtained for the lowest pulse duration tested: 5 μs with a corresponding field amplitude of 3.5 kV·cm^{-1}.

It must be noted that the energy consumption should not be the only criterion to select pulse width and electric field intensity. It was indeed shown in the literature that the pulse width impacts the size of the pores created by the treatment; short pulses result in a multiplicity of small pores while long pulses result in a few large pores [32]. Moreover, the use of micro-pulses, with a duration inferior to 100 μs remains quite unexplored and may have unexpected intracellular effects such as impacting cells viability [33].

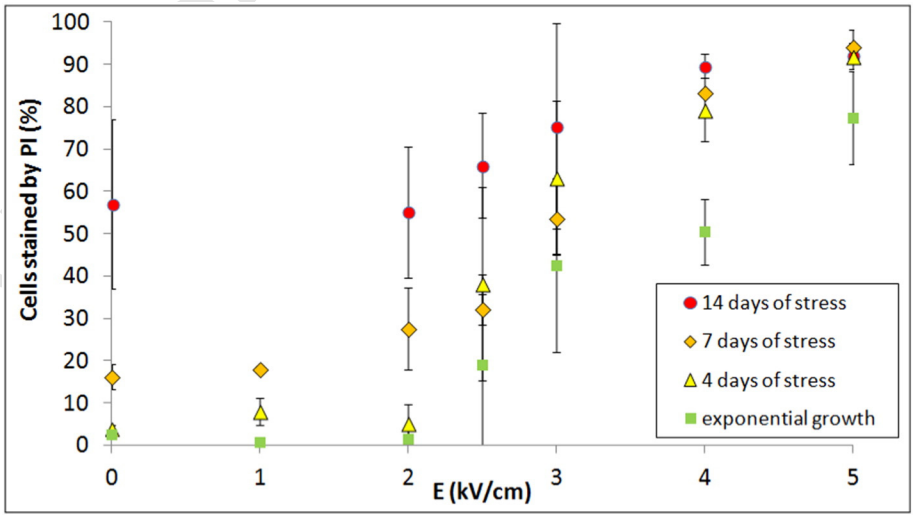

Fig. 6. Permeabilization efficiency of *Chlamydomonas reinhardtii* cells (wild type) over electrical field intensity (PEF treatment conditions: 10 unipolar pulses, 5 μs long, 10 Hz). The efficiency is expressed as the total number of stained cells by PI after treatment (this includes the PI stained cells prior to PEF) over the total number of cells in the sample. The colors correspond to different conditions: normal growth (green square), 4 days of stress (yellow triangle), 7 days of stress (orange diamond) and 14 days of stress (red circle). (For interpretation of the references to color in this figure legend, the reader is referred to the web version of this article.)

Please cite this article as: P. Bodénès, et al., Microdevice for studying the *in situ* permeabilization and characterization of *Chlamydomonas reinhardtii* in lipid accumulation phase..., Algal Res. (2015), http://dx.doi.org/10.1016/j.algal.2016.03.023

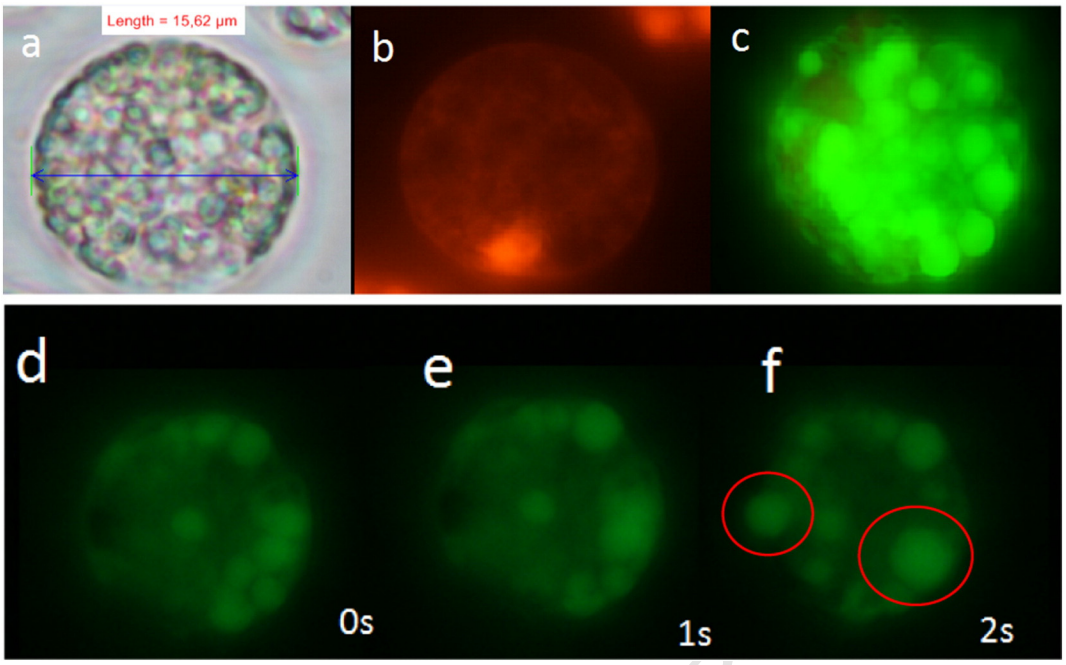

Fig. 7. *Chlamydomonas reinhardtii* (wild type) permeabilized by a PEF treatment of 6 kV·cm^{-1}. (a) bright field, (b) PI detected using CY3 fluorescence filter, (c) lipid droplets stained with bodipy 505/515 using B2A fluorescence filter. Observation at the beginning of the treatment (d), 1 s after (e) and 2 s after (f). Displacement and appearance of large droplets are observed (red circles). Lipid displacement and fusion of intracellular lipid droplets can be observed in a video provided in supplementary data. (For interpretation of the references to color in this figure legend, the reader is referred to the web version of this article.)

3.3. Sensitivity of *C. reinhardtii* cells to PEF at different stages of lipid accumulation

C. reinhardtii at different stages of lipid accumulation (after 4, 7 and 14 days of stress conditions) and in exponential growth phase has been subjected to PEF treatment (burst of 10 unipolar pulses of 5 µs with a frequency of 10 Hz and an amplitude ranging from 0 to 5 kV·cm^{-1}). Results showed that *C. reinhardtii* cell permeabilization occurred at electric field intensities ranging from 2 to 5 kV·cm^{-1} (Fig. 6).

Without PEF treatment (0 kV/cm) and in the case of cells at exponential growth and after 4 days of stress, the percentage of cells stained by PI (Fig. 6) is below 5%. Permeability achieves values in the range of 10 to 20% after 7 days of stress, and dramatically increases above 40% after 14 days of stress. These results show that *C. reinhardtii* cells are naturally permeabilized depending on the time of application and the starvation stress condition.

Furthermore, lipid accumulation does not seem to affect the permeabilization threshold. Indeed after 4, 7 or 14 days of stress, E_{50} remains within the range of 3–3.5 kV·cm^{-1} despite the expected reduction (by a factor of 6) of the cytoplasm conductivity under these conditions, as mentioned in reference [36].

In addition, we found that the cells in exponential growth seem to be less sensitive to the treatment. The difference is mostly notable for 4 kV·cm^{-1}; the total number of cells stained by propidium iodide after PEF treatment was 50.5 ± 7.8% for exponential growth conditions, while more than 80% of the total cells were stained under stress conditions. This difference in cell behavior may be explained by the difference in the size of cells between day 0 and day 4 (see

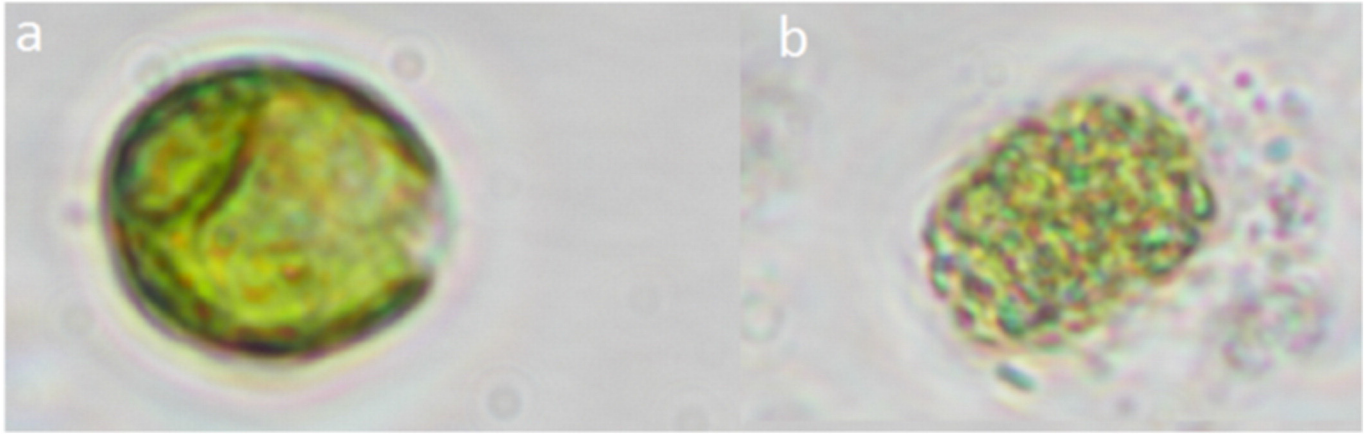

Fig. 8. *Chlamydomonas reinhardtii* cell wall deficient mutant in exponential growth conditions (a) before and (b) 2 min after 6 kV·cm^{-1} treatment.

Please cite this article as: P. Bodénès, et al., Microdevice for studying the *in situ* permeabilization and characterization of *Chlamydomonas reinhardtii* in lipid accumulation phase..., Algal Res. (2015), http://dx.doi.org/10.1016/j.algal.2016.03.023

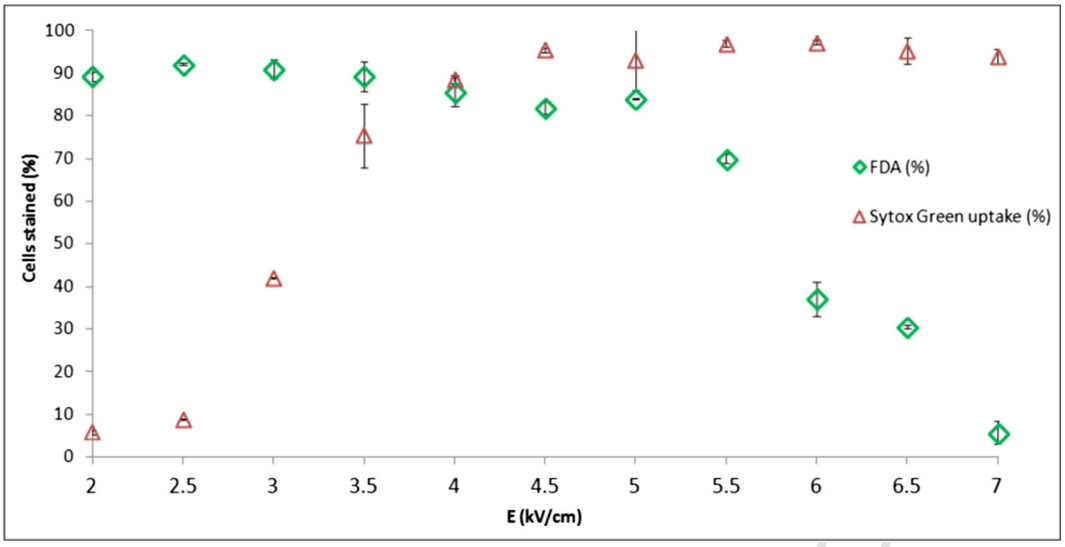

Fig. 9. Red triangle — permeability (measured by Sytox Green uptake) during electroporation in cuvettes; green diamond — enzymatic activity (measured by FDA staining, 1 h after treatment). Treatment: burst of 10 pulses, 10 Hz, pulse duration: 5 μs, cells: *Chlamydomonas reinhardtii* after 7 days of stress. (For interpretation of the references to color in this figure legend, the reader is referred to the web version of this article.)

Section 3.1, Fig. 2), which affects the permeabilization threshold (Eq. (1), Section 1.3).

3.4. Qualitative observations

PI staining of *C. reinhardtii* cells (Fig. 7b) after PEF treatment (6 $kV \cdot cm^{-1}$, burst of 5 μs 10 Hz unipolar pulses) demonstrates membrane permeabilization. However, the cell structure was maintained as suggested by the bright field observation (Fig. 7a). In addition, bodipy fluorescence showed that the lipid droplets remain in the cytoplasm (Fig. 7c). The cell wall may prevent lipid exit from the cytoplasm or cell disintegration even after electrical treatment.

However, a rearrangement of lipid droplets in the cytoplasm was observed a few seconds after the PEF treatment (Fig. 6, d = 0 s, e = 1 s, f = 2 s after treatment); some droplets have merged 2 s after treatment. Lipid displacement and fusion of lipid droplets within the cytoplasm can be observed in real time during the PEF treatment in a video provided in supplementary data. On the whole, observations performed at repeated times in bright and fluorescence fields showed that very short pulses (5 μs) permeabilize the cytoplasm membrane (shown by PI penetration) with limited effects on the cell wall (Fig. 6a), but with clear additional effects on the intracellular lipids.

In addition, the effects of PEF were also tested on a cell wall deficient strain (SAG 34.98) (Fig. 8).

A strong effect on cell integrity was observed in the mutant compared with the wild type strain (Fig. 8). This experiment underlines the fact that when a cell is permeabilized, the cell wall maintains the cell integrity (Fig. 7.a), while a cell wall deficient strain, as *C. reinhardtii* cw15, is disintegrated in such fields (Fig. 8) [56].

3.5. Permeability and viability after PEF treatment

Results show that 50% of cells were permeabilized for electrical fields ranging from 3 to 3.5 $kV \cdot cm^{-1}$ (Fig. 9, sytox green uptake experiment), which is in agreement with data in Fig. 6. Besides, we could demonstrate that the enzymatic activity, measured through fluorescein diacetate (FDA), is affected by electric fields higher than 5 $kV \cdot cm^{-1}$. Particularly at 7 $kV \cdot cm^{-1}$ where more than 90% of the cells have lost their enzymatic activity after 1 h of PEF treatment.

Interestingly, although cell permeabilization occurs at electrical fields ranging from 3 to 5 $kV \cdot cm^{-1}$, data show that cells recover from the electrical stress and are able to keep their enzymatic activity at least for 1 h after the treatment.

Further studies will be undertaken to confirm these results and optimize the process.

3.6. Lipid extraction from permeabilized cells, preliminary results

Previous works already demonstrated enhancement of lipid extraction thanks to electroporation ([15,27]), but with other algae strains (respectively *Ankistrodesmus falcatus* and *C. vulgaris*), and with other electrical conditions (respectively E = 45 $kV \cdot cm^{-1}$ for Δt_{pu} = 360 ns and E = 2.7 $kV \cdot cm^{-1}$ for Δt_{pu} = 100 μs).

We performed preliminary experiments to evaluate the potential of PEF treatment to improve lipid extraction by solvents, under our conditions. *C. reinhardtii* cells harvested after 20 days of nitrogen stress (cells full of lipid droplets) were electroporated (5 μs pulse duration, 7 $kV \cdot cm^{-1}$). Bodipy fluorescence of the non-treated cells, PEF-treated cells, solvent-treated cells and of cells treated by both PEF and solvent were measured and compared. Bodipy fluorescence was reduced by a factor of 1.7 after 20 min of solvent exposure, and by a 4.5 factor after treatment by both PEF and solvent exposure. We interpret this higher florescence reduction as an effect of PEF treatment towards the facilitation of lipid extraction. This preliminary experiment shows that the electroporation treatment may ease the lipid extraction performed by solvent. Further studies will be undertaken to confirm these results and optimize the process.

4. Conclusion

The effect of PEF treatment on microalgae cells was observed and quantified in real-time using a specifically designed microdevice. With this dedicated microdevice, it was possible to (1) estimate the permeabilization threshold for various treatment conditions (electric field amplitude, pulses duration, and number), (2) evaluate the sensitivity of microalgae cells from different culture conditions to PEF and (3) analyze the PEF treatment at the microalgae cell scale, synchronized with the PEF application.

C. reinhardtii, the chosen microalgae strain, was attractive for this study because, as confirmed by our results, this strain is particularly sensitive to PEF (Schwan equation [34]), thanks to the large diameter of the cell (approximately 7–10 μm) compared with many other strains used for lipid production and extraction.

The energy of the PEF technology cost was estimated; the use of short pulses with high field intensity seems to be more favorable. This choice also results in lower heat effects.

Visualization of lipid droplets during the treatment showed their clear displacement in the cytoplasm, and droplets merging in some cases. To the best of our knowledge, this is the first demonstration of lipid droplets behavior under an electrical field. Nevertheless, there was no lipid leakage out of the cell and no cell lysis, even though cells were permeabilized as confirmed by PI or Sytox Green uptake.

These results suggest that electroporation can be used as a pre-treatment of microalgae in order to improve extractions by weakening the cell membrane. Extraction remains challenging for large molecules extractions such as triacylglycerols. However, mild electroporation, as a pre-treatment, might enhance the efficiency of solvent extractions since membrane permeabilization would improve the diffusion of a solvent across the membrane.

Acknowledgments

Q4 The authors acknowledge project funding: ENS Cachan-Université Paris Saclay, CentraleSupélec-Université Paris Saclay, Laboratoire d'excellence LaSIPS, AlgImpact project, Institut d'Alembert, Alguelec project and CNRS.

Appendix A. Supplementary data

Supplementary data to this article can be found online at http://dx.doi.org/10.1016/j.algal.2016.03.023.

References

[1] A.P. Batista, L. Gouveia, N.M. Bandarra, J.M. Franco, A. Raymundo, Comparison of microalgal biomass profiles as novel functional ingredient for food products, Algal Res. 2 (2013) 164–173, http://dx.doi.org/10.1016/j.algal.2013.01.004.
[2] M. Koller, A. Muhr, G. Braunegg, Microalgae as versatile cellular factories for valued products, Algal Res. 6 (2014) 52–63, http://dx.doi.org/10.1016/j.algal.2014.09.002.
[3] G. Breuer, P.P. Lamers, D.E. Martens, R.B. Draaisma, R.H. Wijffels, Effect of light intensity, pH, and temperature on triacylglycerol (TAG) accumulation induced by nitrogen starvation in *Scenedesmus obliquus*, Bioresour. Technol. 143 (2013) 1–9, http://dx.doi.org/10.1016/j.biortech.2013.05.105.
[4] Q. Hu, M. Sommerfeld, E. Jarvis, M. Ghirardi, M. Posewitz, M. Seibert, et al., Microalgal triacylglycerols as feedstocks for biofuel production: perspectives and advances, Plant J. 54 (2008) 621–639, http://dx.doi.org/10.1111/j.1365-313X.2008.03492.x.
[5] Y. Chisti, Biodiesel from microalgae, Biotechnol. Adv. 25 (2007) 294–306, http://dx.doi.org/10.1016/j.biotechadv.2007.02.001.
[6] P.M. Slegers, B.J. Koetzier, F. Fasaei, R.H. Wijffels, G. van Straten, a.J.B. van Boxtel, A model-based combinatorial optimisation approach for energy-efficient processing of microalgae, Algal Res. 5 (2014) 140–157, http://dx.doi.org/10.1016/j.algal.2014.07.004.
[7] J.E. Coons, D.M. Kalb, T. Dale, B.L. Marrone, Getting to low-cost algal biofuels: a monograph on conventional and cutting-edge harvesting and extraction technologies, Algal Res. 6 (2014) 250–270, http://dx.doi.org/10.1016/j.algal.2014.08.005.
[8] S. Sathe, Culturing and Harvesting Marine Microalgae for the Large-scale Production of Biodiesel, (n.d.).
[9] J.W. Richardson, M.D. Johnson, R. Lacey, J. Oyler, S. Capareda, Harvesting and extraction technology contributions to algae biofuels economic viability, Algal Res. 5 (2014) 70–78, http://dx.doi.org/10.1016/j.algal.2014.05.007.
[10] M. Mubarak, a. Shaija, T.V. Suchithra, A review on the extraction of lipid from microalgae for biodiesel production, Algal Res. (2014) http://dx.doi.org/10.1016/j.algal.2014.10.008.
[11] J. Iqbal, C. Theegala, Microwave assisted lipid extraction from microalgae using biodiesel as co-solvent, Algal Res. 2 (2013) 34–42, http://dx.doi.org/10.1016/j.algal.2012.10.001.
[12] Y.-H. Kim, S. Park, M.H. Kim, Y.-K. Choi, Y.-H. Yang, H.J. Kim, et al., Ultrasound-assisted extraction of lipids from *Chlorella vulgaris* using [Bmim][MeSO4], Biomass Bioenergy 56 (2013) 99–103, http://dx.doi.org/10.1016/j.biombioe.2013.04.022.
[13] M. Vanthoor-Koopmans, R.H. Wijffels, M.J. Barbosa, M.H.M. Eppink, Biorefinery of microalgae for food and fuel, Bioresour. Technol. 135 (2013) 142–149, http://dx.doi.org/10.1016/j.biortech.2012.10.135.
[14] O. Parniakov, F.J. Barba, N. Grimi, L. Marchal, S. Jubeau, N. Lebovka, et al., Pulsed electric field and pH assisted selective extraction of intracellular components from microalgae *Nannochloropsis*, Algal Res. 8 (2015) 128–134, http://dx.doi.org/10.1016/j.algal.2015.01.014.
[15] M.D.A. Zbinden, B.S.M. Sturm, R.D. Nord, W.J. Carey, D. Moore, H. Shinogle, et al., Pulsed electric field (PEF) as an intensification pretreatment for greener solvent lipid extraction from microalgae, Biotechnol. Bioeng. 110 (2013) 1605–1615, http://dx.doi.org/10.1002/bit.24829.
[16] S. Haberl, D. Miklavcic, G. Sersa, W. Frey, B. Rubinsky, Cell membrane electroporation—part 2: the applications, IEEE Electr. Insul. Mag. 29 (2013) 29–37, http://dx.doi.org/10.1109/MEI.2013.6410537.
[17] T.S. Santra, P. Wang, Electroporation Based Drug Delivery and its Applications, 2013.
[18] M.L. Yarmush, A. Golberg, G. Serša, T. Kotnik, D. Miklavčič, Electroporation-based technologies for medicine: principles, applications, and challenges, Annu. Rev. Biomed. Eng. 16 (2014) 295–320, http://dx.doi.org/10.1146/annurev-bioeng-071813-104622.
[19] R. Buckow, S. Ng, S. Toepfl, Pulsed electric field processing of orange juice: a review on microbial, enzymatic, nutritional, and sensory quality and stability, Compr. Rev. Food Sci. Food Saf. 12 (2013) 455–467, http://dx.doi.org/10.1111/1541-4337.12026.
[20] M.F. Turk, C. Billaud, E. Vorobiev, A. Baron, Continuous pulsed electric field treatment of French cider apple and juice expression on the pilot scale belt press, Innovative Food Sci. Emerg. Technol. 14 (2012) 61–69, http://dx.doi.org/10.1016/j.ifset.2012.02.001.
[21] L. Schrive, G. Lumia, F. Pujol, N. Boussetta, Liquid food pasteurization by pulsed electric fields: dimensionless analysis via Sherwood number for a comprehensive understanding, Eur. Food Res. Technol. 239 (2014) 707–718, http://dx.doi.org/10.1007/s00217-014-2268-y.
[22] G. Saldaña, I. Álvarez, S. Condón, J. Raso, Microbiological aspects related to the feasibility of PEF technology for food pasteurization, Crit. Rev. Food Sci. Nutr. 54 (2014) 1415–1426, http://dx.doi.org/10.1080/10408398.2011.638995.
[23] K. Loginova, M. Loginov, E. Vorobiev, N.I. Lebovka, Better lime purification of sugar beet juice obtained by low temperature aqueous extraction assisted by pulsed electric field, LWT Food Sci. Technol. 46 (2012) 371–374, http://dx.doi.org/10.1016/j.lwt.2011.10.005.
[24] E. Puértolas, O. Cregenzán, E. Luengo, I. Alvarez, J. Raso, Pulsed-electric-field-assisted extraction of anthocyanins from purple-fleshed potato, Food Chem. 136 (2013) 1330–1336, http://dx.doi.org/10.1016/j.foodchem.2012.09.080.
[25] J. Sheng, R. Vannela, B.E. Rittmann, Evaluation of cell-disruption effects of pulsed-electric-field treatment of synechocystis PCC 6803, Environ. Sci. Technol. 45 (2011) 3795–3802, http://dx.doi.org/10.1021/es103339x.
[26] M. Goettel, C. Eing, C. Gusbeth, R. Straessner, W. Frey, Pulsed electric field assisted extraction of intracellular valuables from microalgae, Algal Res. 2 (2013) 401–408, http://dx.doi.org/10.1016/j.algal.2013.07.004.
[27] K. Flisar, S.H. Meglic, J. Morelj, J. Golob, D. Miklavcic, Testing a prototype pulse generator for a continuous flow system and its use for *E. coli* inactivation and microalgae lipid extraction, Bioelectrochemistry 100 (2014) 44–51, http://dx.doi.org/10.1016/j.bioelechem.2014.03.008.
[28] E. Luengo, S. Condón-Abanto, I. Alvarez, J. Raso, Effect of pulsed electric field treatments on permeabilization and extraction of pigments from *Chlorella vulgaris*, J. Membr. Biol. 247 (2014) 1269–1277, http://dx.doi.org/10.1007/s00232-014-9688-2.
[29] M. Coustets, N. Al-Karablieh, C. Thomsen, J. Teissié, Flow process for electroextraction of total proteins from microalgae, J. Membr. Biol. 246 (2013) 751–760, http://dx.doi.org/10.1007/s00232-013-9542-y.
[30] M.M. Bahi, M.-N. Tsaloglou, M. Mowlem, H. Morgan, Electroporation and lysis of marine microalga *Karenia brevis* for RNA extraction and amplification, J. R. Soc. Interface 8 (2011) 601–608, http://dx.doi.org/10.1098/rsif.2010.0445.
[31] T. Kotnik, P. Kramar, G. Pucihar, D. Miklavcic, M. Tarek, Cell membrane electroporation—part 1: the phenomenon, IEEE Electr. Insul. Mag. 28 (2012) 14–23, http://dx.doi.org/10.1109/MEI.2012.6268438.
[32] G. Saulis, R. Saulė, Size of the pores created by an electric pulse: microsecond vs millisecond pulses, Biochim. Biophys. Acta 1818 (2012) 3032–3039, http://dx.doi.org/10.1016/j.bbamem.2012.06.018.
[33] J.C. Weaver, K.C. Smith, A.T. Esser, R.S. Son, T.R. Gowrishankar, A brief overview of electroporation pulse strength-duration space: a region where additional intracellular effects are expected, Bioelectrochemistry 87 (2012) 236–243, http://dx.doi.org/10.1016/j.bioelechem.2012.02.007.
[34] P. Marszalek, Schwan Equation and Transmembrane Potential Induced by, Vol. 581990 1053–1058.
[35] B.G. Frank, S. Barnes, Biological and Medical Aspects of Electromagnetic Fields (Handbook of Biological Effects of Electromagnetic Fields) 3Ed, 2006.
[36] M.S. Bono, B. a Ahner, B.J. Kirby, Detection of algal lipid accumulation due to nitrogen limitation via dielectric spectroscopy of *Chlamydomonas reinhardtii* suspensions in a coaxial transmission line sample cell, Bioresour. Technol. 143 (2013) 623–631, http://dx.doi.org/10.1016/j.biortech.2013.06.040.
[37] Y. Polevaya, I. Ermolina, M. Schlesinger, B.Z. Ginzburg, Y. Feldman, Time domain dielectric spectroscopy study of human cells. II. Normal and malignant white blood cells, Biochim. Biophys. Acta 1419 (1999) 257–271, http://dx.doi.org/10.1007/BF00188038.
[38] S.J. Beebe, N.M. Sain, W. Ren, Induction of cell death mechanisms and apoptosis by nanosecond pulsed electric fields (nsPEFs), Cells 2 (2013) 136–162, http://dx.doi.org/10.3390/cells2010136.
[39] M.G. Moisescu, M. Radu, E. Kovacs, L.M. Mir, T. Savopol, Changes of cell electrical parameters induced by electroporation. A dielectrophoresis study, Biochim. Biophys. Acta 1828 (2013) 365–372, http://dx.doi.org/10.1016/j.bbamem.2012.08.030.
[40] L. Chopinet, C. Roduit, M.-P. Rols, E. Dague, Destabilization induced by electropermeabilization analyzed by atomic force microscopy, Biochim. Biophys. Acta 1828 (2013) 2223–2229, http://dx.doi.org/10.1016/j.bbamem.2013.05.035.
[41] C.M. Electropermeabilization, An Experimental Evaluation of the Critical Potential Difference, Vol. 651993 409–413.
[42] J. Morren, B. Roodenburg, S.W.H. de Haan, Electrochemical reactions and electrode corrosion in pulsed electric field (PEF) treatment chambers, Innovative Food Sci.

Emerg. Technol. 4 (2003) 285–295, http://dx.doi.org/10.1016/S1466-8564(03)00041-9.
[43] M.P.C. Gustavo, V. Barbosa-Canovas, Maria S. Tapia, Novel Food Processing Technologies, 2004.
[44] M. Kanduser, M. Sentjurc, D. Miklavcic, The temperature effect during pulse application on cell membrane fluidity and permeabilization, Bioelectrochemistry 74 (2008) 52–57, http://dx.doi.org/10.1016/j.bioelechem.2008.04.012.
[45] P.T. Vernier, Z. a Levine, Y.-H. Wu, V. Joubert, M.J. Ziegler, L.M. Mir, et al., Electroporating fields target oxidatively damaged areas in the cell membrane, PLoS One 4 (2009) e7966, http://dx.doi.org/10.1371/journal.pone.0007966.
[46] M.B. Fox, D.C. Esveld, a Valero, R. Luttge, H.C. Mastwijk, P.V. Bartels, et al., Electroporation of cells in microfluidic devices: a review, Anal. Bioanal. Chem. 385 (2006) 474–485, http://dx.doi.org/10.1007/s00216-006-0327-3.
[47] K. Kim, J.A. Kim, S.-G. Lee, W.G. Lee, Seeing the electroporative uptake of cell-membrane impermeable fluorescent molecules and nanoparticles, Nanoscale 4 (2012) 5051, http://dx.doi.org/10.1039/c2nr30578j.
[48] W. Longsine-Parker, H. Wang, C. Koo, J. Kim, B. Kim, A. Jayaraman, et al., Microfluidic electro-sonoporation: a multi-modal cell poration methodology through simultaneous application of electric field and ultrasonic wave, Lab Chip 13 (2013) 2144–2152, http://dx.doi.org/10.1039/c3lc40877a.
Q10 [49] TAP Medium, http://www.chlamy.org/TAP.html. (n.d.).
[50] T. Govender, L. Ramanna, I. Rawat, F. Bux, BODIPY staining, an alternative to the Nile red fluorescence method for the evaluation of intracellular lipids in microalgae, Bioresour. Technol. 114 (2012) 507–511, http://dx.doi.org/10.1016/j.biortech.2012.03.024.
[51] C.I. Trainito, O. Français, B. Le Pioufle, E.N. Supérieure, L. Satie, C.I. Trainito, et al., Monitoring the permeabilization of a single cell in a microfluidic device, through the estimation of its dielectric properties based on combined dielectrophoresis and electrorotation in-situ experiments. Abbreviation : PEF : Pulsed Electric Field, ROT, (n.d.) 1–18. doi:10.1002/elps.201400482.This. Q11
[52] P. Hyka, S. Lickova, P. Přibyl, K. Melzoch, K. Kovar, Flow cytometry for the development of biotechnological processes with microalgae, Biotechnol. Adv. 31 (2012) 2–16, http://dx.doi.org/10.1016/j.biotechadv.2012.04.007.
[53] M.H.a. Michels, A.J. van der Goot, N.-H. Norsker, R.H. Wijffels, Effects of shear stress on the microalgae *Chaetoceros muelleri*, Bioprocess Biosyst. Eng. 33 (2010) 921–927, http://dx.doi.org/10.1007/s00449-010-0415-9.
[54] F.C. Mortimer, D.J. Mason, V. a Gant, Flow Cytometric Monitoring of Antibiotic-Induced Injury in *Escherichia coli* Using Cell-Impermeant Fluorescent Probes, Vol. 442000 676–681, http://dx.doi.org/10.1128/AAC.44.3.676-681.2000.Updated.
[55] V.H. Work, R. Radakovits, R.E. Jinkerson, J.E. Meuser, L.G. Elliott, D.J. Vinyard, et al., Increased lipid accumulation in the *Chlamydomonas reinhardtii* sta7-10 starchless isoamylase mutant and increased carbohydrate synthesis in complemented strains, Eukaryot. Cell 9 (2010) 1251–1261, http://dx.doi.org/10.1128/EC.00075-10.
[56] R.J. Thompson, J.P. Davies, G. Mosig, 'Dark-Lethality' of Certain *Chlamydomonas reinhardtii* Strains is Prevented by Dim Blue Light, 1985 903–907.
[57] M. Siaut, S. Cuiné, C. Cagnon, B. Fessler, M. Nguyen, P. Carrier, et al., Oil accumulation in the model green alga *Chlamydomonas reinhardtii*: characterization, variability between common laboratory strains and relationship with starch reserves, BMC Biotechnol. 11 (2011) 7, http://dx.doi.org/10.1186/1472-6750-11-7.

Please cite this article as: P. Bodénès, et al., Microdevice for studying the *in situ* permeabilization and characterization of *Chlamydomonas reinhardtii* in lipid accumulation phase..., Algal Res. (2015), http://dx.doi.org/10.1016/j.algal.2016.03.023